

AD-A248 992



AEOSR-TR- 92 0235

2

INVESTIGATION OF THE  
INTERFACE PHENOMENA DUE TO  
INTERACTION OF HIGH INTENSITY  
STRESS WAVES WITH  
GEOLOGIC BOUNDARIES

**UTD INCORPORATED**

8560 CINDERBED ROAD  
SUITE 1300  
P O BOX 8560  
NEWINGTON, VIRGINIA 22122  
703 339-0800



**DISTRIBUTION STATEMENT A**  
Approved for public release  
Distribution Unlimited

AIR FORCE OF CONCEPTS RESEARCH (AFRCO)  
NOTICE: This report is the property of the AFRCO and is  
not to be distributed outside the AFRCO. AFRCO Form 150-12

Approved for public release

**DTIC**  
**SELECTE**  
**APR 17 1992**  
**S B D**

92-09746



92 4 15 111

INVESTIGATION OF THE  
INTERFACE PHENOMENA DUE TO  
INTERACTION OF HIGH INTENSITY  
STRESS WAVES WITH  
GEOLOGIC BOUNDARIES

by

Ali Amini  
Steven I. Majtenyi

November, 1991

UTD, Incorporated  
8560 Cinderbed Road, Suite 1300  
Newington, VA 22122

Prepared for

Air Force Office of Scientific Research  
Bolling Air Force Base  
Washington, D.C. 20332

Contract No. F49620-91-C-0008

# REPORT DOCUMENTATION PAGE

*Form Approved*  
**OMB No. 0704-0188**

Public reporting burden for this collection of information is estimated to average 1 hour per response, including the time for reviewing instructions, searching existing data sources, gathering and maintaining the data needed, and completing and reviewing the collection of information. Send comments regarding this burden estimate or any other aspect of this collection of information, including suggestions for reducing this burden, to Washington Headquarters Services, Directorate for Information Operations and Reports, 1215 Jefferson Davis Highway, Suite 1204, Arlington, VA 22202-4302, and to the Office of Management and Budget, Paperwork Reduction Project (0704-0188), Washington, DC 20503.

1. AGENCY USE ONLY (Leave blank)		2. REPORT DATE 30 November 1991		3. REPORT TYPE AND DATES COVERED Annual 1 Nov 90 - 30 Nov 91	
4. TITLE AND SUBTITLE Investigation Of The Interface Phenomena Due To Interaction Of High Intensity Stress Waves With Geologic Boundaries				5. FUNDING NUMBERS Contract No. F49620-91-C-0008  <b>2302/CS</b>	
6. AUTHOR(S) Ali Amini Steven I. Majtenyi					
7. PERFORMING ORGANIZATION NAME(S) AND ADDRESS(ES) UTD, Incorporated 8560 Cinderbed Road, Suite 1300 Newington, VA 22122				8. PERFORMING ORGANIZATION REPORT NUMBER  OSR-9008	
9. SPONSORING/MONITORING AGENCY NAME(S) AND ADDRESS(ES) Air Force Office of Scientific Research Bolling AFB, D.C. 20332-6448				10. SPONSORING/MONITORING AGENCY REPORT NUMBER <b>F49620-91-C-0008</b>	
11. SUPPLEMENTARY NOTES					
12a. DISTRIBUTION/AVAILABILITY STATEMENT  <b>unlimited</b>				12b. DISTRIBUTION CODE	
13. ABSTRACT (Maximum 200 words)  During the reporting period a stress-strain relationship was derived for the study of the interface phenomena when a high intensity stress wave impinges on a geologic boundary. The derived relationship was based on the ultimate density concept, i.e., the density of the material increases non-linearly with increasing stresses approaching a limiting value before a polymorphic phase transformation occurs.  The derived stress-strain relationship was compared with high pressure data for three rock types. Based on this comparison it was determined that the derived stress-strain relationship modeled material behavior accurately with realistic physical parameters. The relationship was then used in the solution of second order non-linear Partial Differential Equations (PDE) of motion. The method of similarity was used to transform the non-linear PDE to an Ordinary Differential Equation (ODE). The ODE was then solved by standard techniques. The result was a closed form equation for particle displacement profiles in space and time domains including particle velocity acceleration and stress profiles. These profiles will be used in <span style="float: right;">(continued on back)</span>					
14. SUBJECT TERMS High Intensity Pressure Wave      Polymorphic Phase Transformation Geologic Boundary Ultimate Density				15. NUMBER OF PAGES 34	
17. SECURITY CLASSIFICATION OF REPORT Unclassified				16. PRICE CODE	
18. SECURITY CLASSIFICATION OF THIS PAGE Unclassified		19. SECURITY CLASSIFICATION OF ABSTRACT Unclassified		20. LIMITATION OF ABSTRACT	

CLASSIFIED BY:

DECLASSIFY ON:

Abstract - continued:

upcoming tasks to determine the role of various parameters in the generation of new waves at interfaces with mediums of finite thickness and the response at interfaces which can be described by a half-space.

TABLE OF CONTENTS

	<u>Page</u>
1.0 INTRODUCTION.....	1
2.0 MATERIAL BEHAVIOR UNDER INCREASING STRESSES.....	3
3.0 PROGRESS REPORT.....	7
3.1 General.....	7
3.2 Progress, Task a, Material Model Selection.....	7
3.2.1 <u>Derivation of Exponential Stress-Strain</u> <u>Relationships</u> .....	10
3.2.2 <u>Determination of Material Parameters</u> .....	13
3.3 Progress, Task b, Equations of Motion.....	18
4.0 ANALYSIS OF THE INTERFACE PHENOMENA.....	24
5.0 CONCLUDING REMARKS.....	26
6.0 REFERENCES.....	28

1  
1975  
10/20

<b>Accession For</b>	
NTIS GRA&I	<input checked="" type="checkbox"/>
DTIC TAB	<input type="checkbox"/>
Unannounced	<input type="checkbox"/>
Justification	
By _____	
Distribution/	
Availability Codes	
Dist	Avail and/or Special
A-1	

LIST OF FIGURES

	<u>Page</u>
Figure 1. Structure of geologic materials.....	3
Figure 2. Behavior of geologic materials under increasing stresses.....	5
Figure 3. Stress-density diagram for geologic materials.....	6
Figure 4. State of stress in the shockwave.....	10
Figure 5. Stress-density data fit for gray granodiorite.....	15
Figure 6. Stress-density data fit for NTS tuff.....	16
Figure 7. Stress-density data fit for limestone.....	17
Figure 8. x-y and x'- y' coordinate systems.....	19
Figure 9. Solution of equations at the interface.....	25

LIST OF TABLES

	<u>Page</u>
Table 1. Number of material parameters for elastic-plastic constitutive models.....	9
Table 2. Stress-strain data for three rocks.....	14

## LIST OF NOTATIONS

A	-	Compressibility Parameter
B	-	Physical Parameter
C	-	Physical Parameter
E	-	Initial Young's Modulus
F	-	Displacement Function
G	-	Displacement Function
H	-	Displacement Function
$K_0$	-	Coefficient of Lateral Stress
R	-	Physical Parameter
V	-	Instantaneous Volume
$V_0$	-	Initial Volume
e	-	2.7183
l	-	Particle Displacement
t	-	time axis
u	-	Particle Velocity in x direction
v	-	Particle Velocity in y direction
x	-	Coordinate axis
y	-	Coordinate axis
$\Delta V/V$	-	Volumetric Strain
$\partial$	-	Partial Derivative
$\epsilon$	-	Normal Strain
$\phi$	-	Angle of Internal Friction
$\rho$	-	Instantaneous Density
$\rho_0$	-	Initial Density
$\rho_{ult}$	-	Ultimate Density
$\sigma$	-	Major Principal Stress
$\sigma_x$	-	Normal Stress in x direction
$\sigma_y$	-	Normal Stress in y direction
$\tau_{xy}$	-	Shear Stress



## 1.0 INTRODUCTION

The objective of this program is to study the phenomena associated with impinging of high intensity pressure waves at geologic discontinuities. This includes wave refraction, reflection, and generation of new waves at the interface. The interface separates two geologic materials with different physical properties. The geologic materials are assumed to be made up of solid particles with air filled macroscopic voids in between. The solid particles may be in simple or welded and cemented contact.

High intensity pressure waves are generated in underground nuclear and, to a lesser extent, in conventional explosions. In the vicinity of the explosion, the ground shockwave deforms the surrounding material to such an extent that the material behaves like a fluid (hydrodynamic region). The discontinuities in this region are diffused and have minimal effects on ground shock propagation. At greater distances from the explosion source, the shockwave is converted to a high intensity pressure wave. The geologic material traversed by this high intensity pressure wave absorbs some of the energy of the wave by deforming, remolding, and compressing to high densities. Eventually, at sufficiently long distances from the working point, the high intensity pressure wave loses enough energy to propagate like a seismic wave with minimal disturbance of the geologic material (seismic zone).

The interface phenomena in the seismic region is well understood and reliable analytic models exist for their analysis. However, in the transition zone, between hydrodynamic and seismic regions, the interface phenomena is not understood clearly and solutions based on seismic or hydrodynamic conditions extended into this region yield unsatisfactory results. As a result, the focus of this study is on studying and understanding of the interface phenomena in the transition zone. The nature of the research effort is to obtain a basic understanding of the phenomena. As a result, there is an emphasis on development of analytic solutions that clearly show the role of the various parameters. For this purpose, the following research effort is planned to be carried out over a 3 year period:

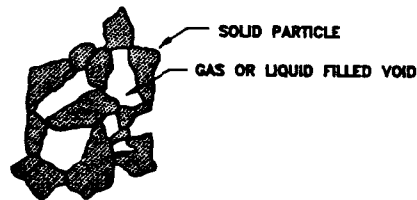
- a. Select a stress-strain relationship for modeling of material behavior over the pressure range existing in the transition zone.
- b. Solve the equations of motion at the interface of two different materials using the newly selected stress-strain relationships.
- c. Perform a sensitivity analysis to determine the effects of various parameters on solutions obtained in task b. Then ensure that the solutions converge to seismic and hydrodynamic equations at low and high pressures respectively.
- d. Analyze the new mechanical waves other than reflected and refracted waves generated at interfaces at all stress levels.
- e. Model the material response at interfaces considering geometric factors, material characteristics and particle displacement intensities.

In the following sections the behavior of materials at increasing stresses is reviewed. Then the progress made in tasks a and b is presented and the results discussed. After the discussion, means of using the obtained results in achieving the objectives of the program are presented.

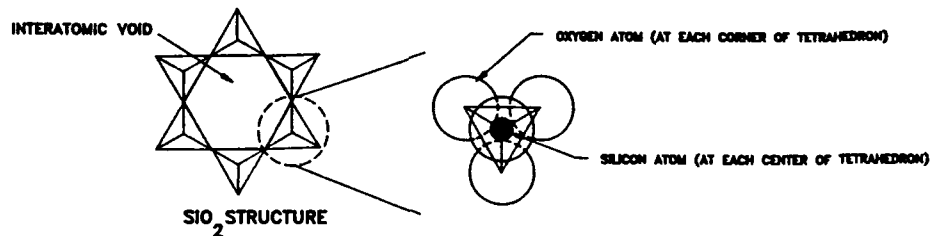
## 2.0 MATERIAL BEHAVIOR UNDER INCREASING STRESSES

Geologic materials consist of solid particles packed together with varying degrees of gas or liquid filled voids. In granular soils the particles are uncemented, whereas in rocks a cementing material binds the particles together. The solid particles that provide the rigidity of geologic materials are made up of crystalline minerals with interatomic voids. Figure 1 shows the macroscopic and microscopic structure of a typical geologic material.

- GEOLOGIC MATERIALS CONSIST OF SOLID PARTICLES WITH GAS OR LIQUID FILLED VOIDS



- SOLID PARTICLES ARE MADE UP OF CRYSTALLINE MINERALS WITH INTERATOMIC VOIDS



ALKS100

Figure 1. Structure of geologic materials.

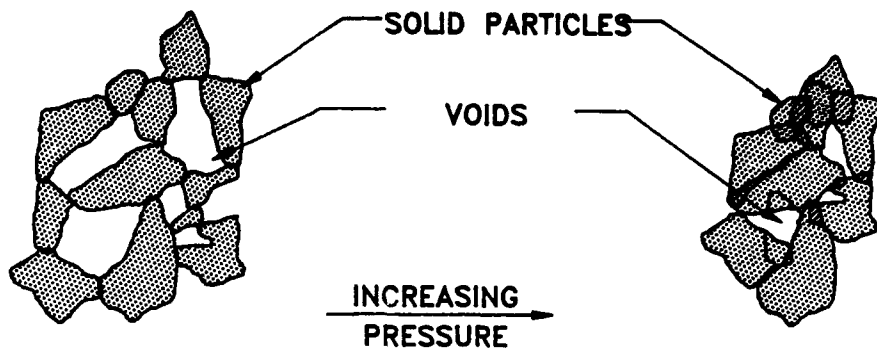
As the external stresses on a geologic material increase, the contact between solid particles is broken, the particles slide, and stress concentrations arise at particle to particle contact points. In response, the particles crush and readjust themselves to minimize stress concentration. This leads to closure and collapse of the voids between the

solid particles. In addition to particle crushing and readjustment, the molecules making up the crystalline cells compress and the interatomic voids decrease in size. The overall result of grain sliding, crushing, inter-particle void closure, and inter-atomic void reduction is an increase in the density of the material. However, as the voids decrease in size, increasingly larger stresses are required to compress the material.

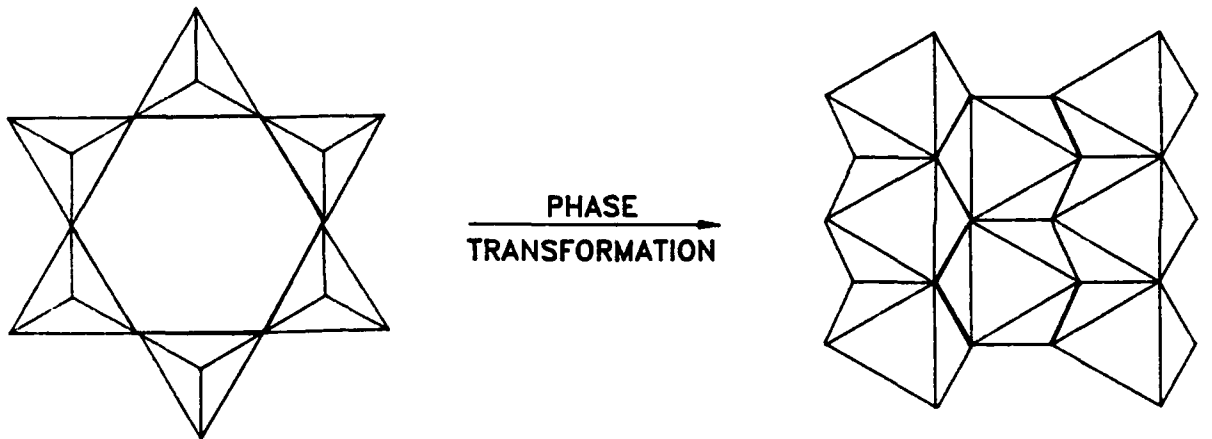
At low stresses, the dominant compression mechanism is that of grain sliding, readjustment, crushing and inter-particle void closure. However, at high stresses most of the inter-particle voids are closed and crystalline compression and interatomic void closure dominate. If stresses are high enough, after most of the inter-particle voids are collapsed, a polymorphic phase transformation occurs in the crystalline structure of the particles. The compression then continues by closure of the new inter-particle voids and interatomic voids in the new crystalline phase. Figure 2 shows the compression mechanism of a geologic material made up primarily of quartz particles.

The stress-density relationship for compression of geologic materials to high pressures is shown in Figure 3. As shown in the figure, the density,  $\rho$ , increases with stress,  $\sigma$  (major principal stress), but the rate of density increase slows with increasing stress and  $\rho$  tends towards a limiting value  $\rho_{ult}$  (ultimate density). If the stresses continue to increase, there will be a discontinuity in the  $\sigma$  vs.  $\rho$  diagram corresponding to crystalline phase transformation. It is worth noting that an actual  $\sigma$  vs.  $\rho$  diagram will not be a smooth curve. Rather, discontinuities may occur at lower stresses due to grain crushing. But in some materials they are minor compared to the discontinuity related to the phase change at higher stresses.

Stresses in the seismic region are on the order of the shear strength of the geologic material. In most cases this corresponds to stresses equal to or less than one kilobar. Stresses in the hydrodynamic region are high enough to overcome material strength, causing it to behave as an incompressible fluid. In most materials this corresponds to stresses on the order of 100 kbars. As a result, the stress range of interest for this study is between 1 and 100 kbars. Over this range of stresses, most



MACROSCOPIC COMPRESSION



SI IN TETRAHEDRAL  
COORDINATION WITH OXYGEN  
(AT LOW PRESSURE)

SI IN OCTAHEDRAL  
COORDINATION WITH OXYGEN  
(AT HIGH PRESSURE)

HEXAGONAL SYMMETRY

TETRAGONAL SYMMETRY

ALKS125

MICROSCOPIC COMPRESSION

Figure 2. Behavior of geologic materials under increasing stresses.

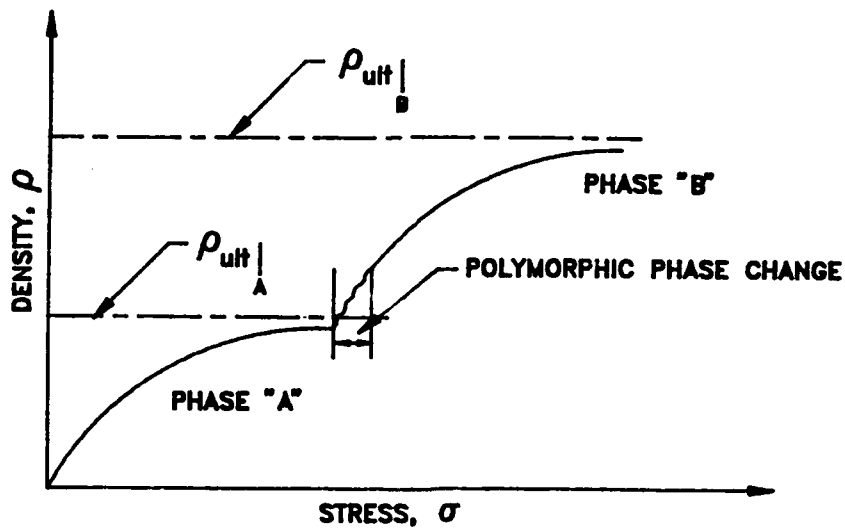


Figure 3. Stress-density diagram for geologic materials.

geologic materials are expected to behave as shown in Figure 3; therefore, the selected material model for interface study has to incorporate the concept of limiting or ultimate density.

### 3.0 PROGRESS REPORT

#### 3.1 General

The work accomplished during the first year of the contract was related to tasks a and b. Under task a, published stress strain relationships were reviewed in order to combine a suitable relationship with one based upon the ultimate density concept. The stress-strain relationship was then derived and compared to high pressure experimental data for various rocks.

Under task b, the equations of motion were written for a particle at the interface. The equations incorporated the non-linear stress-strain relationship developed in task a. The resulting equations were second order non-linear partial differential equations. Various schemes were devised to solve these equations analytically. At present, work is continuing on task b to generate additional solutions for the equations of motion and determine their physical reality.

The following sections summarize the work accomplished in tasks a and b.

#### 3.2 Progress, Task a, Material Model Selection

The nature of the contract work is basic research; therefore, it is of particular interest to understand the role of the physical variables involved in the interface phenomena. The best approach to this understanding is the development of a mathematical model for the interaction process between the high intensity pressure wave and the interface using a material model with physical parameters. The outcome of the mathematical model will be a set of analytic functions describing particle displacement, velocity, acceleration and stress profiles in space and time domains.

As expected, the equations of motion leading to the desired profiles were non-linear, coupled with non-linear material behavior. Therefore, it was necessary to use a stress-strain relationship with the fewest test determined parameters that could model material behavior over the pressure

range of interest. Most stress-strain relationships for geologic materials have numerous parameters that have to be determined from laboratory tests under quasi-static conditions. Geologic materials under high rate dynamic loading may behave in a totally different manner than they do under quasi-static conditions. This was another important factor that dictated the selection of a material model with the fewest test determined parameters. However, great care was exercised to not sacrifice reality for the sake of simplicity.

The ideal approach to selection of an appropriate stress-strain relationship would be to develop exact relationships for ground materials at any state of stress. However, this objective would not be realistic in view of the present state-of-the-art and the historical evolution of stress-strain relationships. Highly sophisticated relationships exist in the low stress intensity range, but the level of sophistication and the number of models decrease with increasing stress intensities. For the purpose of this project, published stress-strain relationships were reviewed to select the one that could be combined with the ultimate density concept so as to include the entire stress regime encountered in the vicinity of an underground explosion.

Published stress-strain relationships for geologic materials (granular soil, and rocks) can be grouped into five general categories: Elastic, Elasto-plastic, polynomial, hyperbolic, and exponential. Elastic stress-strain relationships model material behavior at low stresses using generalized Hook's law. The material density in elastic relationships increases with increasing stresses without a limit.

Elastic-plastic stress-strain relationships mathematically describe material behavior in the elastic range and beyond the yield condition of the material. These relationships utilize a yield criterion as the start of plastic deformations. Beyond yield, plastic deformations are calculated by various flow rules. Numerous flow rules and elastic-plastic relationships are developed for geologic materials. The emphasis in development of elastic-plastic relationships is to incorporate an increasing number of material parameters in order to develop more exact stress-strain relationships to be used in numerical modeling.



The elastic-plastic relationships reviewed under this task are listed in Table 1 along with the number of material parameters that have to be determined from laboratory experiments [1,2,3].

Table 1. Number of material parameters for elastic-plastic constitutive models.

Constitutive Model	Material Parameters
Elastic-Perfectly Plastic	8
Modified AFWL	37
Effective Stress Cap	19
Lade	21
ARA Conic	31

The major disadvantage of using elastic-plastic models in the analytic study of the interface phenomena is the large number of material parameters and the fact that most of the parameters do not have physical meaning.

Polynomial, hyperbolic, and exponential stress-strain relationships represent the non-linear behavior of geologic materials by assuming a parabolic, quadratic, hyperbolic, or exponential relationship between stresses and strains. The assumed relationships are closed form and have only two or three test determined parameters. In the present study, an exponential relationship was assumed to exist between stresses and strains with the exponential parameters related to the compressibility and the ultimate density of the material.

### 3.2.1 Derivation of Exponential Stress-Strain Relationships

Under task a, exponential stress-strain relationships for general three dimensional (isotropic and deviatoric) states of stress were developed based on the ultimate density concept. However, in wave propagation studies when the wave front is flat (as shown in Figure 4) it is realistic to assume that the lateral strains inside the pressure wave are zero (uniaxial strain compression). This assumption simplifies the relationships significantly without introducing large uncertainties. As shown in Figure 4, the lateral stress required to prevent lateral movement is  $K_0\sigma$ , where  $\sigma$  is the major principal stress, and  $K_0$  is the lateral stress coefficient.  $K_0$  is related to the angle of internal friction of the material,  $\phi$ :

$$K_0 = 1 - \sin \phi \quad (1)$$

At high stresses the shear strength of the material approaches zero, and  $K_0$  approaches one causing the state of stress to converge to hydrodynamic conditions.

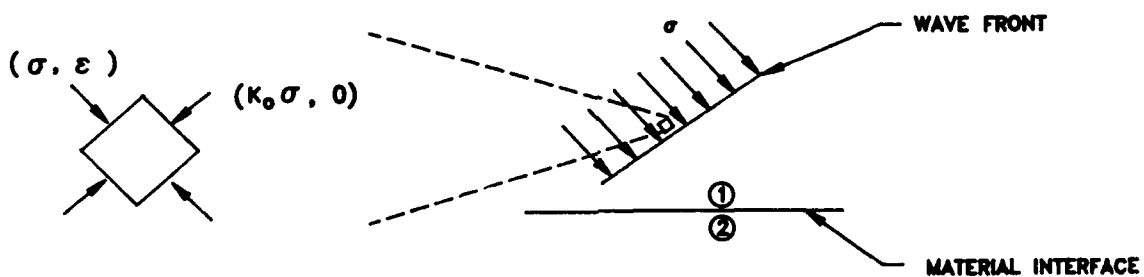


Figure 4. State of stress in the shockwave.

The exponential stress-density relationship used to derive the general and the uniaxial stress-strain relationships was[4]:

$$\rho = \rho_{ult} - (\rho_{ult} - \rho_o) e^{-A\sigma} \quad (2)$$

where

- $\rho$  - Instantaneous density,
- $\rho_{ult}$  - Ultimate density,
- $\rho_o$  - Initial density,
- $A$  - Compressibility parameter, and
- $\sigma$  - Major principal stress

the compressibility parameter is also related to the initial modulus of elasticity of the material, E:

$$A = \frac{1}{E(R - 1)} \quad (3)$$

where

$$R = \frac{\rho_{ult}}{\rho_o} \quad (4)$$

In cases where a polymorphic phase transformation occurs inside the stress range of interest, Eq. (2) will be discontinuous. As shown in Figure 3, the material parameters for the two phases will be different, leading to two pressure density relationships with different  $\rho_{ult}$  and A.

Eq. (2) can be rearranged in terms of the major principal stress  $\sigma$ :

$$\sigma = - \frac{1}{A} \ln \left( \frac{R - \frac{\rho}{\rho_o}}{R - 1} \right) \quad (5)$$

In the uniaxial compression of a mass of material, the density-volume relationship is:

$$\text{constant} = \rho V = \rho_0 V_0 \quad (6)$$

where  $V$  and  $V_0$  are the instantaneous and the initial volume of the material, respectively. Note that in compression  $V < V_0$ . Denoting the volumetric strain,  $\Delta V/V$  as:

$$\frac{\Delta V}{V} = \frac{V_0 - V}{V} \quad (7)$$

Eq. (6) may be written in the following form, which requires no approximation:

$$\rho = \rho_0 \left( 1 + \frac{\Delta V}{V} \right) \quad (8)$$

Under uniaxial strain conditions, the strain in the direction of propagation,  $\epsilon$  is equal to the volumetric strain, which leads to the following density-strain relationship:

$$\rho = \rho_0 (1 + \epsilon) \quad (9)$$

Substituting Eq. (9) in Eq. (5) leads to the following stress-strain relationship:

$$\sigma = - \frac{1}{A} \ln (1 - C\epsilon) \quad (10)$$

where

$$C = \frac{\rho_o}{\rho_{ult} - \rho_o} \quad (11)$$

Eq. (10) was the stress-strain relationship used in the solution of the equations of motion in task b.

### 3.2.2 Determination of Material Parameters

Material parameters for the selected stress-strain relationship (Eq. 10) are  $\rho_{ult}$  and A. They can be determined from experiments that measure stress as a function of volumetric strain. For the purpose of this study, literature related to high pressure experiments on geologic materials was reviewed, and data for three rock types that had sufficient data points over the stress range of interest were identified. The three rock types were dry NTS tuff, gray granodiorite, and limestone, [5] and [6]. The data obtained in Ref. [5] were obtained from high pressure die assemblies up to 45 kbars. However, the data in [6] were obtained from high explosive laboratory tests generating pressures over 68 kbars. The reason for using data from two different experiments was the lack of data in any single experiment that would cover the entire stress range of interest, (1 - 100 kbars). Table 2 presents the data for each rock type. The data points were used along with Eq. (2) to determine  $\rho_{ult}$  and A by the method of least squares. The results are shown in Figures 5 - 7.

The data fit analysis for granodiorite resulted in two curves passing through the data points. The first curve passes through the data points up to 68 kbars, and the second curve passes through the points of over 123 kbars stress. The reason for the discontinuity between 68 and 123 kbars could be explained by a polymorphic phase transformation in the quartz crystals making up the rock. The phase transformation in quartz is commonly seen, where quartz transforms to stishovite. As reported by Swegle in his study of irreversible phase transitions and wave propagation in silicate geologic materials [7], "the phase transformation does not take place under

Table 2. Stress-strain data for three rocks.

Rock Type	Reference	Stress(kb)	Vol. Strain % $\Delta V/V$	Density ( $\text{kg/m}^3$ )
Gray granodiorite	[5]	5.0	0.9	2694
	[5]	10.0	1.8	2718
	[5]	15.0	2.7	2740
	[5]	25.0	4.3	2785
	[5]	35.0	5.8	2824
	[5]	42.0	6.7	2850
	[6]	68.0	9.3	2918
	[6]	123.0	17.2	3129
	[6]	148.0	26.4	3375
	[6]	182.0	32.3	3532
Limestone	[5]	5.0	10.5	2543
	[5]	10.0	16.8	2688
	[5]	15.0	20.6	2776
	[5]	25.0	26.7	2919
	[5]	35.0	29.4	2979
	[5]	44.0	30.9	3011
	[6]	130.0	38.2	3180
NTS Tuff	[5]	5.0	4.5	2342
	[5]	10.0	7.1	2400
	[5]	15.0	9.2	2445
	[5]	25.0	12.6	2523
	[5]	35.0	15.9	2596
	[5]	46.0	19.2	2670
	[6]	74.0	40.2	2792
	[6]	109.0	46.4	3116
[6]	181.0	48.5	3240	

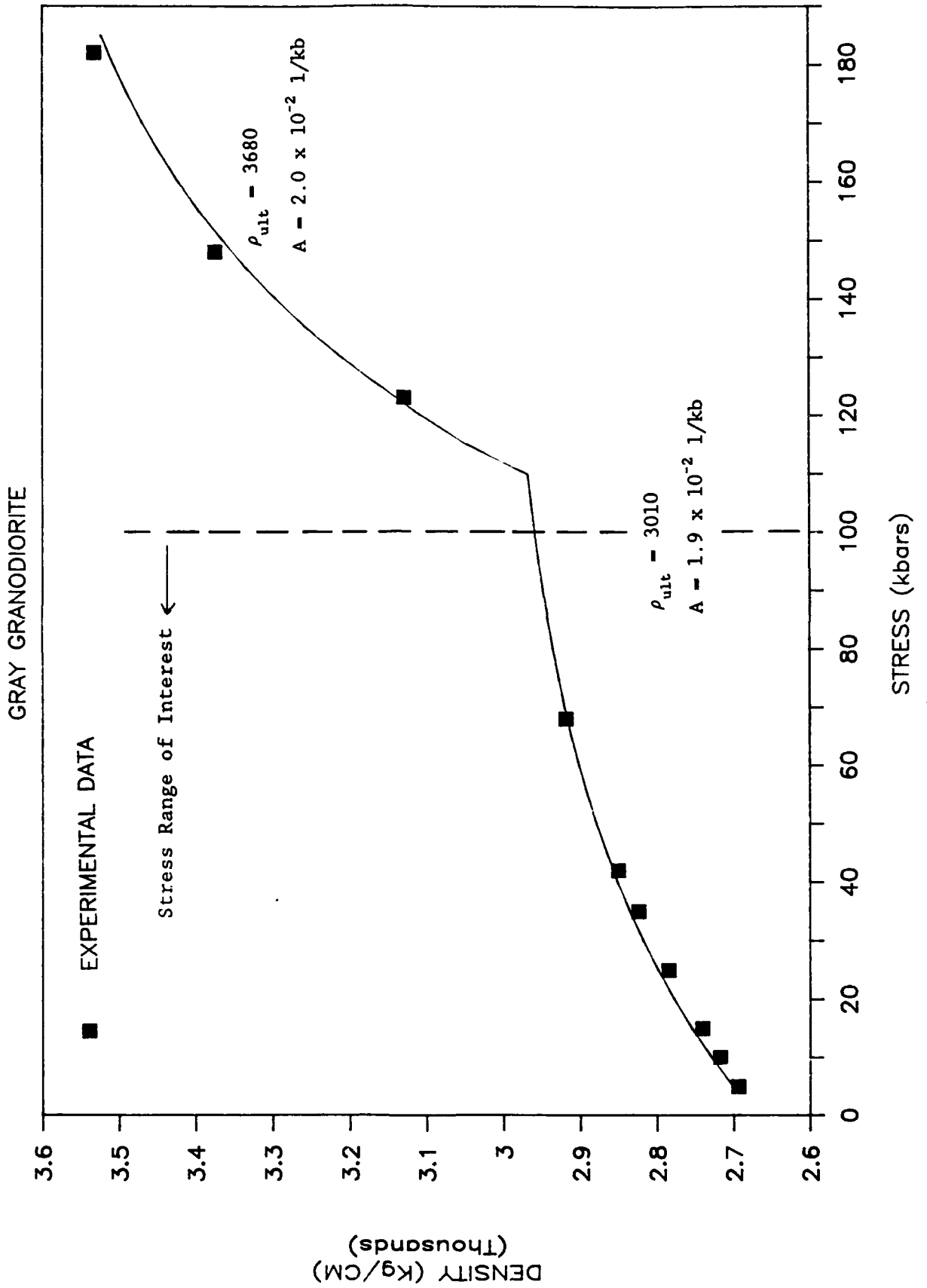


Figure 5. Stress-density data fit for gray granodiorite.

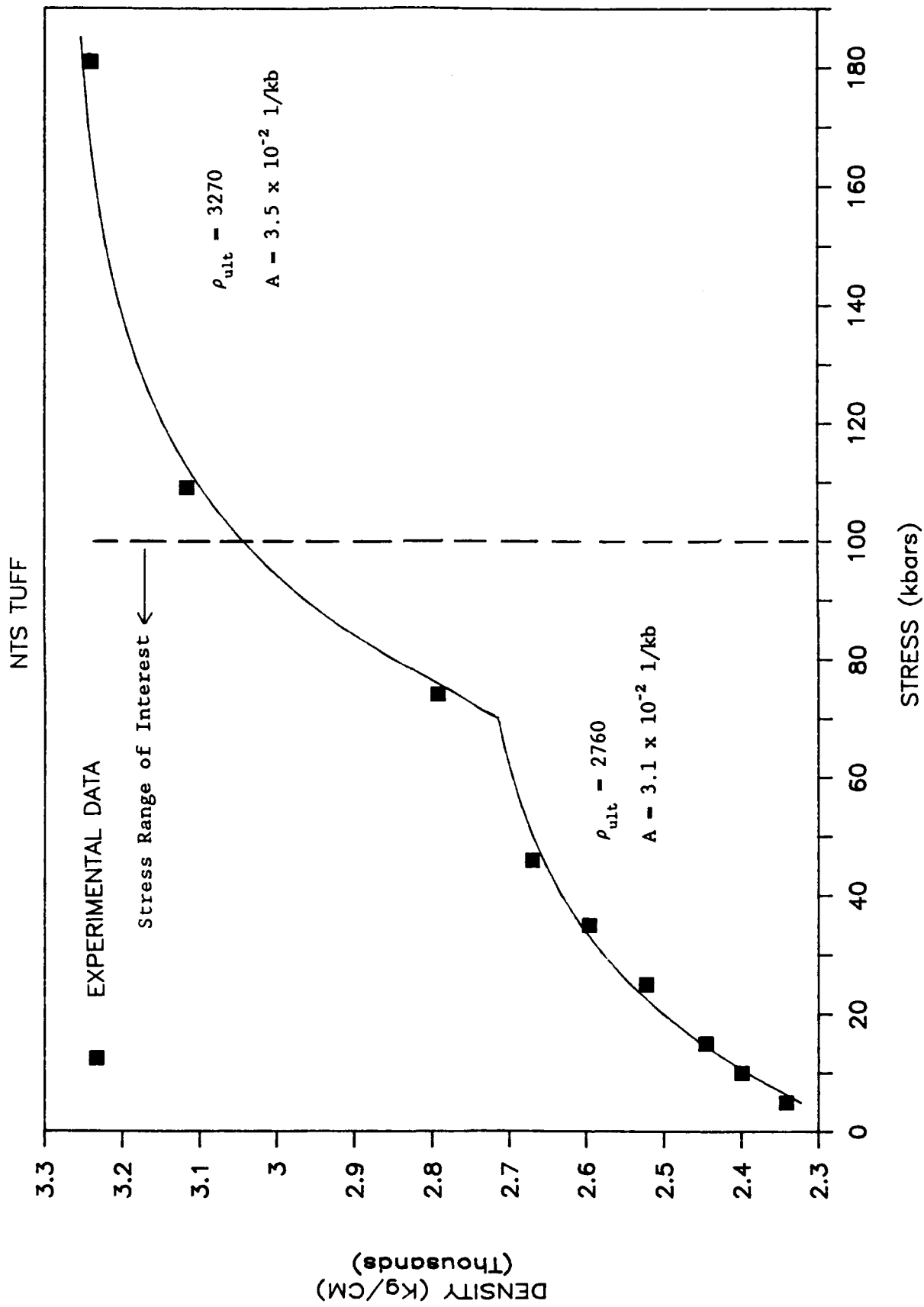


Figure 6. Stress-density data fit for NTS tuff.



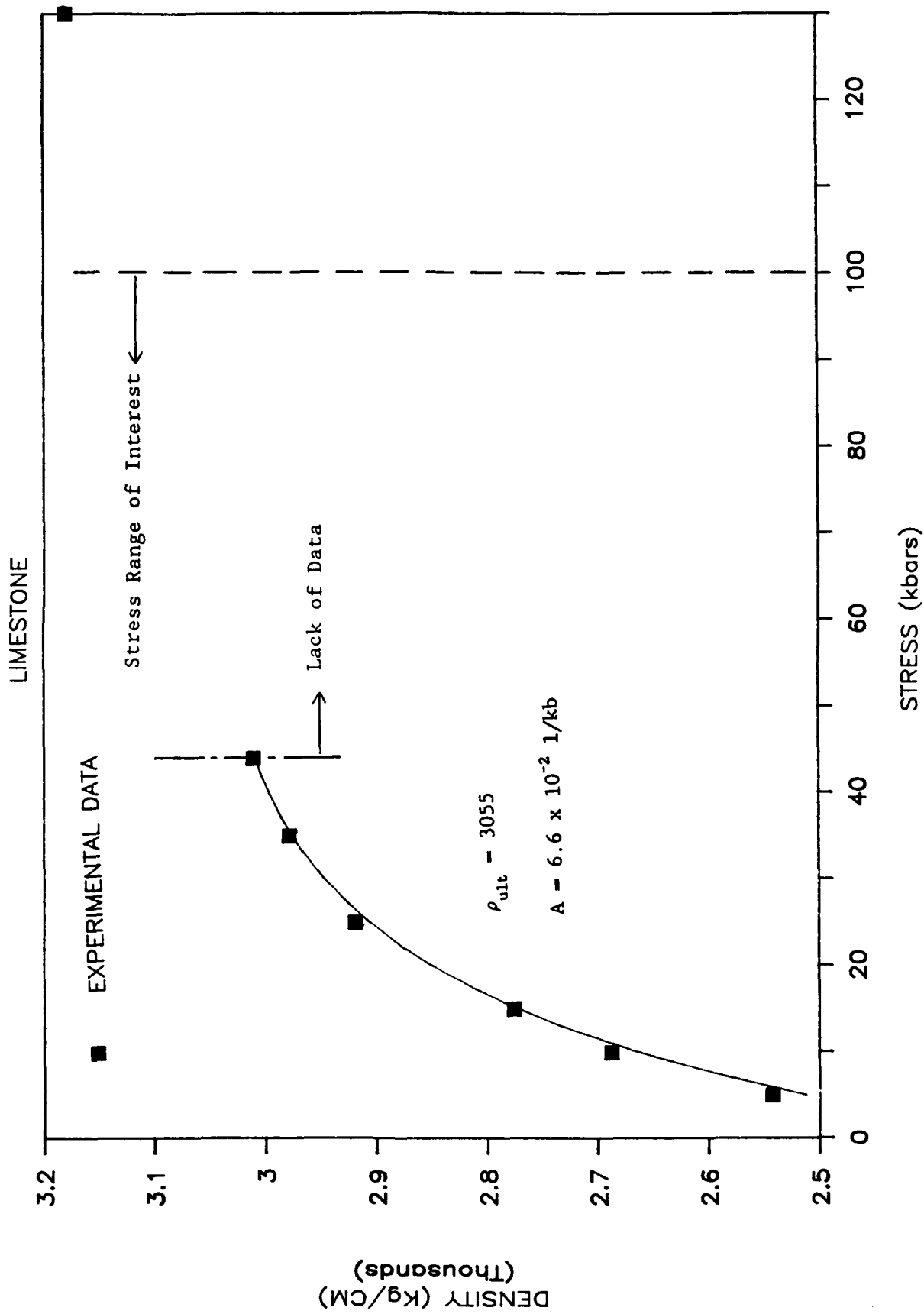


Figure 7. Stress-density data fit for limestone.

conditions of thermodynamic equilibrium, but rather through a metastable mixed phase region spanning several tens of GPa between the onset and completion of the transition", [8]. Referring to Figure 5, the phase transformation starts in the vicinity of 100 kbars with further compression due to the reduction of interatomic voids as phase transformation continues.

The same phenomenon of phase transformation occurred in compression of the tuff sample, but at stresses in the range of 70 kbars. The difference in phase transformation stresses in tuff and granodiorite is that tuff is made up of mostly zeolite minerals which undergo phase transformation at lower stresses than the quartz mineral.

Tests carried out on limestone produced a sufficient number of data points up to 44 kbars, but not enough data points beyond 44 kbars to result in a reliable second curve fit where one would expect a polymorphic phase transformation.

The above data analysis shows that accurate material modeling is possible with stress-volumetric strain data covering the entire stress range of interest. The analysis also indicates that in materials where phase changes occur inside the stress range of interest two sets of material parameters have to be determined. The first data set will be primarily due to macroscopic void closure and the second set will be related to interatomic void closure and crystalline phase transformation.

### 3.3 Progress, Task b, Equations of Motion

In order to study the interface phenomena, it is necessary to set up equilibrium equations and solve them with the conditions present at the two sides of the interface. The coordinate systems selected for this purpose are shown in Figure 8. The  $x'-y'$  coordinate system is attached to the interface, whereas the  $x-y$  coordinate system travels with the pressure wave. The equilibrium equations are set up and solved in the  $x-y$  system and then transformed to the  $x'-y'$  system.

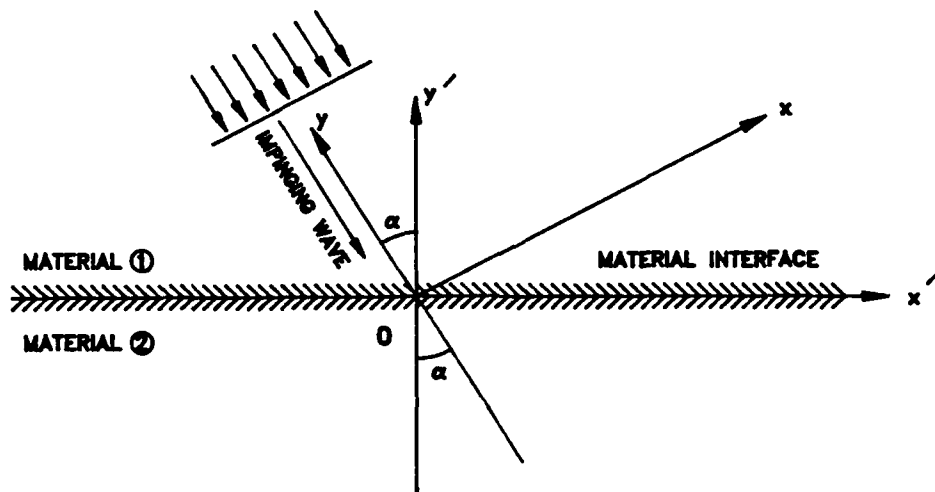


Figure 8. x-y and x'- y' coordinate systems.

Dynamic equilibrium equations in the x-y system are:

$$\text{x direction } \rho \left( \frac{\partial u}{\partial t} + u \frac{\partial u}{\partial x} + v \frac{\partial u}{\partial y} \right) = \frac{\partial \sigma_x}{\partial x} + \frac{\partial \tau_{xy}}{\partial y} \quad (12)$$

$$\text{y direction } \rho \left( \frac{\partial v}{\partial t} + u \frac{\partial v}{\partial x} + v \frac{\partial v}{\partial y} \right) = \frac{\partial \sigma_y}{\partial y} + \frac{\partial \tau_{xy}}{\partial x} \quad (13)$$

where  $u$  and  $v$  - Particle velocity in the  $x$  and  $y$  directions respectively  
 $\sigma_x$  and  $\sigma_y$  - Normal stress in the  $x$  and  $y$  directions respectively  
 $\tau_{xy}$  - Shear stress  
 $t$  - Time variable

Under the condition of uniaxial strain, particle velocity in the  $x$  direction is zero, and in the absence of shear stresses  $\tau_{xy}$  is zero. As a result, the dynamic equilibrium equations are simplified to:

$$\frac{\partial \sigma_x}{\partial x} = 0 \quad (14)$$

$$\rho \left( \frac{\partial v}{\partial t} + v \frac{\partial v}{\partial y} \right) = \frac{\partial \sigma_y}{\partial y} \quad (15)$$

Eq. (14) implies that  $\sigma_x$  is constant in the  $x$  direction and varies as a function of  $y$ :

$$\sigma_x = F(y) = K_0 \sigma_y \quad (16)$$

As a result, solving the equilibrium equation in the  $y$  direction will lead to the solution in the  $x$  direction.

Taking the partial derivative of Eq. (10) with respect to  $y$  leads to:

$$\frac{\partial \sigma}{\partial y} = \frac{BC}{1-C \frac{\partial l}{\partial y}} \frac{\partial^2 l}{\partial y^2} \quad (17)$$

where  $B$  -  $1/\lambda = E(R-1)$ , and  
 $l$  - particle displacement in the  $y$  direction.

The equations for strain, particle velocity and its partial derivatives in terms of particle displacement,  $l$  are:

$$\epsilon = \frac{\partial l}{\partial y} \quad (18)$$

$$v = \frac{\partial l}{\partial t} \quad (19)$$

$$\frac{\partial v}{\partial t} = \frac{\partial^2 l}{\partial t^2} \quad (20)$$

$$\frac{\partial v}{\partial y} = \frac{\partial^2 l}{\partial y \partial t} \quad (21)$$

Substituting Eq. (9), (18), (19), (20), and (21) in Eq. (15) leads to the following equilibrium equation:

$$\rho_o \left( 1 + \frac{\partial l}{\partial y} \right) \frac{\partial^2 l}{\partial t^2} + \rho_o \left( 1 + \frac{\partial l}{\partial y} \right) \frac{\partial l}{\partial t} \frac{\partial^2 l}{\partial y \partial t} - \frac{E}{1-C} \frac{\partial l}{\partial y} \frac{\partial^2 l}{\partial y^2} \quad (22)$$

The above equation is a second order non-linear Partial Differential Equation (PDE) with one dependent variable  $l$ , and two independent variables  $y$  and  $t$ . The solution of Eq. (22) leads to particle displacement profiles in the time and  $y$  coordinates. The velocity, acceleration, and stress profiles can be derived from displacement profiles. These profiles are then used to study the interface phenomena.

Non-linear PDEs have many families of solutions. As a result, one has to ensure that the solutions obtained are physically realistic. This will be done by analyzing the various partial derivatives and profiles and comparison with profiles observed in the field.

At present one solution has been obtained for Eq. (22) based on the similarity method [9, 10]. The purpose of this method is to reduce the number of independent variables and convert the PDE to an ordinary differential equation. The solution obtained is:

$$1 - \frac{2}{3} \frac{1+C}{C} y + F^{1/3} + G^{1/3} \quad (23)$$

where

$$F = \left[ \frac{8}{27} \left( \frac{1+C}{C} \right)^3 y^3 + \frac{4}{C} \frac{E}{\rho_0} t^2 y + H \right]^{1/3} \quad (24)$$

$$G = \left[ \frac{8}{27} \left( \frac{1+C}{C} \right)^3 y^3 + \frac{4}{C} \frac{E}{\rho_0} t^2 y - H \right]^{1/3} \quad (25)$$

$$H = \sqrt{\frac{64}{27} \frac{(1+C)^3}{C^4} \frac{E}{\rho_0} t^2 y^4 + \frac{16}{C^2} \frac{E^2}{\rho_0^2} t^4 y^2} \quad (26)$$

Work is continuing to determine the physical reality of Eq. (23), and also determine if the equation can be simplified further. Each component of Eq. (23) may by itself be a solution to the equilibrium equation. Therefore, instead of Eq. (23), one may be able to use  $1 - F^{1/3}$  or  $G^{1/3}$  as a solution.

Other solutions can also be achieved for Eq. (22) by the method of Legendre transformation [9,10], and Backlund Transformations [11]. At present, a solution based on the method of Legendre transformation is being attempted which transforms the non-linear PDE to a linear PDE with standard solution. The purpose of finding additional solutions is to be able to handle various stress profiles used as an input for the interface study.

#### 4.0 ANALYSIS OF THE INTERFACE PHENOMENA

Analysis of the interface phenomena is the objective of the research program and will be carried out under tasks d and e. Tasks a and b have resulted in equations that describe the various profiles of a high intensity pressure wave at the interface. In task c a sensitivity analysis will be performed to determine the effects of various parameters on the desired profiles in order to ensure the effects are realistic. The solutions will also be studied under stresses typical of those in the seismic and hydrodynamic regions to ensure their convergence to seismic and hydrodynamic solutions.

After completing task c the equations of motion will be solved for particle displacement, velocity and stress at the interface in material 1. Then they will be resolved into components normal and tangent to the interface. Various conditions of continuity at the interface will be applied to displacement, velocities, and stresses in order to determine their magnitudes and directions in material 2. For example, the condition of no slip or partial slip at the interface will determine if the tangential components will be transferred fully or partially into material 2. After the particle displacement, velocity and stress in material 2 are determined, force equilibrium and energy conservation equations will be used to determine the type and magnitude of the waves reflected back into material 1. This process is shown in Figure 9. The purpose of carrying out this exercise is to understand the role of various parameters in the generation of new waves at the interface, and the response of the interface. For example, a comparison of particle displacement in material 1 with the thickness of the interface (if the interface is filled with a material different from those of materials 1 and 2) will determine if one can treat the interface as a plane of discontinuity or the problem has to be solved as a three layer system. Another purpose of tasks d and e is to determine if solutions similar to those used in seismicity based on Snell's law can be developed for the non-linear behavior of the material in the transition region.

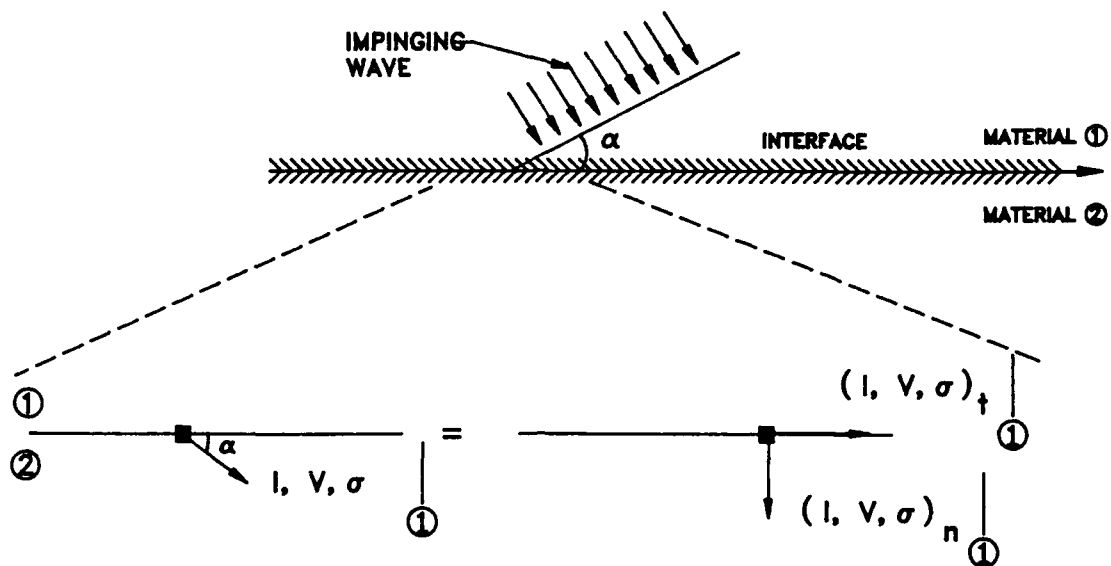


Figure 9. Solution of equations at the interface.



## 5.0 CONCLUDING REMARKS

The research effort carried out during the first year of the program resulted in a stress-strain relationship that models material behavior in the region of interest accurately. The relationship is based on the concept that as a geologic material compresses, its density increases non-linearly and approaches a limiting value. A polymorphic phase transformation may also result over the stress range of interest. The use of this relationship is useful in understanding interface phenomena because it is based on the most significant physical parameters. This is especially advantageous as compared with methods employing coefficients which have no physical significance.

The region of interest (termed the transition zone) in this study lies between the hydrodynamic zone in the immediate vicinity of an underground explosion and the seismic zone far from the explosion where pressure waves do not alter the material. The stresses in the transition zone may range from 1 to 100 kbars. This led to the comparison of the stress-strain relationship with data from experiments that generated stresses in excess of 100 kbars. The results for three rock types indicated that the selected stress-strain relationship fitted the experimental data accurately and led to realistic material parameters.

Another outcome of the research effort was the solution of the equations of motion at the interface using the selected stress-strain relationship. The solution obtained is a closed form equation for the particle displacement profile in space and time. From this profile it is possible to derive the profiles for particle velocity, acceleration, and stresses at the interface. Because the equations of motion are non-linear partial differential equations, they have many families of solutions. At present, work is continuing to obtain other solutions (Lengendre transformation) and then establish their physical reality and ranges of applicability.

The research effort planned for the next reporting period consists of a sensitivity analysis on the obtained solutions and a check on their convergence to seismic and hydrodynamic equations at low and high stresses respectively. Finally, the interface phenomena will be studied using the

derived relationships. The purpose of this study will be to understand the role of various parameters in the generation of new waves at the interface and the response of the interface if it has a finite thickness.

## 6.0 REFERENCES

- [1] Saada, A., and G. Bianchini. CONSTITUTIVE EQUATIONS FOR GRANULAR NON-COHESIVE SOILS. Proc. of the International Workshop on Constitutive Equations for Granular Non-Cohesive Soils, July 1987, Balkema, 1989.
- [2] Nelson, I., M. L. Baron, and I. Sandler. Chapter 13, Mathematic Models for Geologic Materials for Wave-Propagation Studies. Reprinted from SHOCK WAVES AND MATHEMATICAL PROPERTIES OF SOLIDS, Copyright 1971, by Syracuse University Press, Syracuse, N.Y.
- [3] Douglas, M. H., and W. C. Dass. FUNDAMENTAL PROPERTIES OF SOILS FOR COMPLEX DYNAMIC LOADING. Technical Report AFOSR-TR-85-1232, Air Force Office of Scientific Research, 1985.
- [4] Majtenyi, S. I. STRESS-STRAIN RELATIONSHIPS IN COMPRESSION. Volume 1 of 10, UTD Internal Research Reports.
- [5] Stephens, D. R. THE HYDROSTATIC COMPRESSION OF EIGHT ROCKS. J. of Geophysical Research, Vol. 69, No. 14, 1964.
- [6] Lombard, D. B. THE HUGONION EQUATION OF STATE OF ROCKS. Technical Report UCRL-6311, Lawrence Radiation Laboratory, 1961.
- [7] Swegle, J. W. IRREVERSIBLE PHASE TRANSITIONS AND WAVE PROPAGATION IN SILICATE GEOLOGIC MATERIALS. Technical Report. SAND89-1443. UC-404. Sandia National Laboratories, 1989.
- [8] *ibid.*, p. 1.
- [9] Myint-U, T. and L. Debnath. PARTIAL DIFFERENTIAL EQUATIONS FOR SCIENTISTS AND ENGINEERS. 3rd ed., North Holland Publishing. 1987.
- [10] Ames, W. F. NON-LINEAR PARTIAL DIFFERENTIAL EQUATIONS IN ENGINEERING. Vols. I and II. Academic Press, 1965 and 1972.
- [11] Rogers, C., and W. F. Shadwick. BACKLUND TRANSFORMATIONS AND THEIR APPLICATIONS. Academic Press, 1982.